An introduction to microscopic cluster models

D. Baye
Physique Quantique, C.P. 165/82, and
Physique Nucléaire Théorique et Physique Mathématique, C.P. 229,
Université Libre de Bruxelles (ULB), B 1050 Brussels, Belgium

1 Presentation

In nuclear physics, microscopic models take account of all nucleons in a nucleus or a collision. They treat exactly the Pauli antisymmetrization of these nucleons. In non-relativistic microscopic models, all physical results are derived from interaction potentials between nucleons.

The nucleons are described within the isospin formalism. They are thus assumed to have the same nucleon mass m_N. The microscopic Hamiltonian reads

$$H = \sum_{i=1}^{A} \frac{\boldsymbol{p}_i^2}{2m_N} + \sum_{i>j=1}^{A} V_{ij} - T_{\rm CM}, \tag{1}$$

where A is the nucleon or mass number, $\boldsymbol{p}_i$ is the momentum of nucleon i and V_{ij} is the interaction between nucleons i and j. The two-body interactions V_{ij} may involve a nuclear term with central, spin-orbit, tensor and other components, and the Coulomb interaction. Three-nucleon interactions will be neglected here. They are surely needed in calculations with realistic forces and may also be taken into account in cluster models. In Hamiltonian (1), the centre-of-mass (CM) kinetic energy $T_{\rm CM}$ is subtracted to eliminate CM effects from the cluster model.

The microscopic cluster approach is based on an assumed cluster structure, i.e. on the occurrence of correlated subsystems in the fully antisymmetric wave function of the A-nucleon system [1, 2]. The microscopic cluster model provides a unified framework for the description of nuclear spectroscopy and nuclear reactions involving light nuclei. The cluster assumption allows the application of the microscopic model to systems with typically up to $A \sim 20 - 24$, but requires the use of effective nucleon-nucleon two-body interactions which are adapted to the cluster approximation.

Because the interactions are invariant under rotation, Hamiltonian (1) commutes with the total angular-momentum operator

$$\boldsymbol{J} = \boldsymbol{L} + \boldsymbol{S}, \tag{2}$$

where the total orbital-momentum operator $\boldsymbol{L}$ is defined as the sum of the orbital momenta $\boldsymbol{L}_i$ of each nucleon,

$$\boldsymbol{L} = \sum_{i=1}^{A} \boldsymbol{L}_i, \tag{3}$$

and the total spin operator $\boldsymbol{S}$ is defined as the sum of the spins $\boldsymbol{S}_i$ of each nucleon,

$$\boldsymbol{S} = \sum_{i=1}^{A} \boldsymbol{S}_i. \tag{4}$$

Because the interactions are invariant under reflection, H also commutes with the parity operator which reverses the coordinates of all nucleons.

2 Clusters and effective forces

2.1 Cluster wave functions

A cluster is a system of nucleons which are assumed to be correlated within a larger nucleus. This model assumes that clusters are particularly well bound and that the interaction between clusters is weak. However, because of the Pauli antisymmetrization, nucleons do not belong to a definite cluster. A cluster is characterized by its wave function which can be occupied by any nucleon. The cluster structure manifests itself by a deformation of the nucleus. In a microscopic model, this structure may be hidden in some states, when the clusters strongly overlap.

The most typical cluster is the α cluster made of two protons and two neutrons. The free α particle is a well bound system ($B/A \approx 7.07$ MeV) with a small radius. An α cluster may differ from a free α particle within a larger nucleus but the free α particle is a good approximation within the cluster model. Other typical clusters are ^{3}H or ^{3}He although they are less well bound. For heavier nuclei, closed-shell systems such as ^{16}O or ^{40}Ca are also considered as good clusters.

Cluster wave functions are selected within some model. The most used model is the harmonic-oscillator shell model because it possesses a remarkable property: a Slater determinant can be factorized into an internal wave function and a CM wave function. As an example, let us consider the case of the α cluster. The nucleon coordinates are $\boldsymbol{r}_1$ to $\boldsymbol{r}_4$. A Slater determinant in the harmonic-oscillator shell model involves four $0s$ oscillator orbitals corresponding to the different spin and isospin states.

$$\Phi = \frac{1}{\sqrt{4!}} \begin{vmatrix} \varphi(\boldsymbol{r}_1)|+_1 n_1\rangle & \varphi(\boldsymbol{r}_1)|-_1 n_1\rangle & \varphi(\boldsymbol{r}_1)|+_1 p_1\rangle & \varphi(\boldsymbol{r}_1)|-_1 p_1\rangle \\ \varphi(\boldsymbol{r}_2)|+_2 n_2\rangle & \varphi(\boldsymbol{r}_2)|-_2 n_2\rangle & \varphi(\boldsymbol{r}_2)|+_2 p_2\rangle & \varphi(\boldsymbol{r}_2)|-_2 p_2\rangle \\ \varphi(\boldsymbol{r}_3)|+_3 n_3\rangle & \varphi(\boldsymbol{r}_3)|-_3 n_3\rangle & \varphi(\boldsymbol{r}_3)|+_3 p_3\rangle & \varphi(\boldsymbol{r}_3)|-_3 p_3\rangle \\ \varphi(\boldsymbol{r}_4)|+_4 n_4\rangle & \varphi(\boldsymbol{r}_4)|-_4 n_4\rangle & \varphi(\boldsymbol{r}_4)|+_4 p_4\rangle & \varphi(\boldsymbol{r}_4)|-_4 p_4\rangle \end{vmatrix} \tag{5}$$

where $|+\rangle$ and $|-\rangle$ are the two spin states $|sm_s\rangle$ with $s = 1/2$ and $m_s = \pm 1/2$ and $|n\rangle$ and $|p\rangle$ are the two isospin states $|tm_t\rangle$ with $t = 1/2$ and $m_t = \pm 1/2$. The $0s$ harmonic-oscillator orbital is given by

$$\varphi(\boldsymbol{r}) = (\pi b^2)^{-3/4} e^{-r^2/2b^2} \tag{6}$$

where b is the harmonic-oscillator size parameter. The four orbitals appearing in (5) are orthogonal and normed. Hence the Slater determinant is also normed.

Expression (5) can be written more compactly by introducing the antisymmetrization projector of A particles

$$\mathcal{A} = \frac{1}{A!} \sum_p (-1)^p P_p. \tag{7}$$

In this expression, P_p is the operator which performs permutation p and the sum runs over the $A!$ permutations p of the A particles. The notation $(-1)^p$ represents the signature of the permutation, i.e. it is equal to $+1$ for an even permutation and -1 for an odd permutation. A permutation is even or odd according to the parity of any number of exchanges of two particles which realize the permutation. The operators P_p are unitary but, in general, not Hermitian. The antisymmetrization operator (7) is Hermitian

$$\mathcal{A}^\dagger = \mathcal{A}. \tag{8}$$

It is a projector,

$$\mathcal{A}^2 = \mathcal{A}. \tag{9}$$

By using the antisymmetrization projector of 4 particles, expression (5) can also be written as

$$\begin{aligned} \Phi &= \sqrt{4!}\mathcal{A}\varphi(\boldsymbol{r}_1)|+_1 n_1\rangle\varphi(\boldsymbol{r}_2)|-_2 n_2\rangle\varphi(\boldsymbol{r}_3)|+_3 p_3\rangle\varphi(\boldsymbol{r}_4)|-_4 p_4\rangle \\ &= \sqrt{4!}\varphi(\boldsymbol{r}_1)\varphi(\boldsymbol{r}_2)\varphi(\boldsymbol{r}_3)\varphi(\boldsymbol{r}_4)\mathcal{A}|+_1 n_1 -_2 n_2 +_3 p_3 -_4 p_4\rangle \end{aligned} \tag{10}$$

Now let us introduce the CM coordinate

$$\boldsymbol{R}_{\rm CM} = \frac{1}{4}(\boldsymbol{r}_1 + \boldsymbol{r}_2 + \boldsymbol{r}_3 + \boldsymbol{r}_4) \tag{11}$$

and the translation-invariant internal coordinates

$$\boldsymbol{\xi}_i = \boldsymbol{r}_i - \boldsymbol{R}_{\rm CM} \tag{12}$$

which are not independent ($\sum_i \boldsymbol{\xi}_i = 0$). The identity

$$\sum_{i=1}^{4} r_i^2 = 4R_{\rm CM}^2 + \sum_{i=1}^{4} \xi_i^2 \tag{13}$$

allows us to factorize the Slater determinant into

$$\Phi = \varphi_{\rm CM}\phi \tag{14}$$

where the normed CM wave function is defined as

$$\varphi_{\rm CM} = (\pi b^2/A)^{-3/4} e^{-AR_{\rm CM}^2/2b^2} \tag{15}$$

with $A = 4$. The translation-invariant internal wave function

$$\phi = \sqrt{4!}(\pi b^2)^{-3} e^{-(\xi_1^2+\xi_2^2+\xi_3^2+\xi_4^2)/2b^2}\mathcal{A}|+_1 n_1 -_2 n_2 +_3 p_3 -_4 p_4\rangle \tag{16}$$

is thus also normed. The factorization property (14) with the CM wave function (15) remains valid for arbitrary mass numbers A within the harmonic-oscillator shell model provided all shells except the most external one are filled (Bethe and Rose theorem [3]). It plays a crucial role in the cluster model.

The total angular momentum and parity quantum numbers of the α particle are $J^\pi = 0^+$ and its isospin is $T = 0$. The Slater determinant (5) or (10) reproduces these values. Obviously, its total orbital momentum L is equal to zero and its parity is $\pi = +1$. Its total spin and isospin are $S = 0$ and $T = 0$. For example, let us write (10) as

$$\Phi = \mathcal{A}\chi \tag{17}$$

where χ is any term in the expansion of the Slater determinant. The total-spin raising operator $S_+ = \sum_i S_{i+}$ is fully symmetric and commutes with $\mathcal{A}$ which leads to

$$S_+\Phi = \mathcal{A}S_+\chi = 0 \tag{18}$$

because $S_+\chi$ involves two identical states and thus vanishes under antisymmetrization. Hence the maximum projection M_S of the spin is zero and Φ is an eigenstate of $\boldsymbol{S}^2$ corresponding to $S = 0$. A similar argument holds for the isospin $T = 0$.

Having $L = 0$, the cluster state (5) of the α particle is surely not very realistic since it is known that ^{4}He has a significant $L = 2$ component (corresponding to a total spin $S = 2$) due to the tensor force. A variational calculation involving wave function (5) gives very poor results with realistic forces because it does not comply with the repulsive core at short distances and with components such as the tensor force. Hence the cluster model makes use of *phenomenological effective forces* [4, 5] which have a simpler structure and partly compensate the weaknesses of the model wave functions.

2.2 Example of phenomenological effective force

Let us describe the Minnesota effective interaction [5] which does not include tensor forces, but simulates their contribution in the binding energy of the deuteron by the central term. Its central part is given by

$$V = [V_R(r) + \tfrac{1}{2}(1 + P^\sigma)V_t(r) + \tfrac{1}{2}(1 - P^\sigma)V_s(r)][\tfrac{1}{2}u + \tfrac{1}{2}(2 - u)P^M], \tag{19}$$

where u is an adjustable parameter close to unity. In this expression, $\boldsymbol{r} = \boldsymbol{r}_i - \boldsymbol{r}_j$ is the relative coordinate between particles i and j, P^σ is the operator exchanging the spins of these particles and P^M is the Majorana operator exchanging their positions, i.e. transforming their relative coordinate $\boldsymbol{r}$ into $-\boldsymbol{r}$. The operators $\frac{1}{2}(1 + P^\sigma)$ and $\frac{1}{2}(1 - P^\sigma)$ are thus projectors on the triplet ($S = 1$) and singlet ($S = 1$) spin states of nucleons i and j. For $u = 1$, the factor $\frac{1}{2}(1 + P^M)$ projects on even waves only (s, d, ...). Since we are working in the isospin formalism, it is convenient to make the replacement $P^M = -P^\sigma P^\tau$ where P^τ is the operator exchanging the isospins of the nucleons. This relation is a consequence of the identity

$$P^M P^\sigma P^\tau = -1 \tag{20}$$

valid for fully antisymmetric wave functions.

The functions V_k with $k = R$ (repulsive core), t (triplet) and s (singlet) are Gaussians,

$$V_k(r) = V_{0k}e^{-\kappa_k r^2}, \tag{21}$$

Table 1: Parameters V_{0k} (in MeV) and κ_k (in fm^{-2}) of the Minnesota interaction.

k	V_{0k}	κ_k
R	200.0	1.487
t	−178.0	0.639
s	−91.85	0.465

where V_{0k} and κ_k are adjusted parameters (see Table 1). The Minnesota potential provides the correct binding energy 2.22 MeV of the deuteron (without tensor force!) and reproduces fairly well some properties of nucleon-nucleon scattering. It involves the admixture parameter u whose standard value is $u = 1$, but which can be slightly modified to fit one important physical quantity such as the energy of a given state.

This central potential is often complemented by a spin-orbit force such as

$$V_{LS} = -2S_0\hbar^{-2}\nu^{-5}\exp(-r^2/\nu^2)\boldsymbol{L}\cdot(\boldsymbol{S}_i+\boldsymbol{S}_j) \tag{22}$$

with $\boldsymbol{L} = \boldsymbol{r}\times\boldsymbol{p}$ where $\boldsymbol{p} = \frac{1}{2}(\boldsymbol{p}_i - \boldsymbol{p}_j)$ is the relative momentum between the nucleons. Expression (22) has the advantage of remaining valid for $\nu \to 0$. Choosing $\nu = 0$, one eliminates this parameter which is weakly relevant because the spin-orbit force has a shorter range than the central force.

The α-particle energy can be obtained from Hamiltonian (1) involving nuclear interaction (20) and the Coulomb interaction with a variational calculation employing determinant (5) as trial function. It is the given by

$$E_\alpha = \frac{9\hbar^2}{4m_N b^2} + 3\sum_{k=R,t,s}(1+\delta_{kR})V_{0k}\left(\frac{\kappa_k^2}{\kappa_k^2+2b^2}\right)^{3/2} + \sqrt{\frac{2}{\pi}}\frac{e^2}{b} \tag{23}$$

as a function of the oscillator parameter b. The minimum energy −25.58 MeV occurs for $b = 1.28$ fm. The experimental binding energy is 28.296 MeV.

3 Resonating-group method

3.1 Resonating-group wave function

The resonating-group wave function was proposed by Wheeler in 1937 [6]. For a system of two clusters, it can lead to a description of a bound nucleus or a collision between two light nuclei. The clusters represent correlations in bound states or in the overlapping part of scattering states. They describe the colliding nuclei in the asymptotic part of scattering states. As expected from the Pauli antisymmetrization postulate, it is antisymmetrized with respect to all nucleons. It involves the logical but not so intuitive idea that nucleons belonging to different nuclei are antisymmetrized even before the actual collision.

Let us consider A nucleons with total charge Ze distributed into two clusters involving respectively A_1 and A_2 nucleons,

$$A = A_1 + A_2. \tag{24}$$

The charges of the clusters are $Z_1 e$ and $Z_2 e$,

$$Z = Z_1 + Z_2. \tag{25}$$

We first assume that nucleons with coordinates $\boldsymbol{r}_1$ to $\boldsymbol{r}_{A_1}$ belong to cluster 1 and that nucleons with coordinates $\boldsymbol{r}_{A_1+1}$ to $\boldsymbol{r}_A$ belong to cluster 2.

Let us introduce a coordinate system involving the internal coordinates

$$\boldsymbol{\xi}_i^{(1)} = \boldsymbol{r}_i - \boldsymbol{R}_{\rm CM}^{(1)} \qquad (i = 1, \ldots, A_1 - 1) \tag{26}$$

for nucleus 1 and

$$\boldsymbol{\xi}_i^{(2)} = \boldsymbol{r}_i - \boldsymbol{R}_{\rm CM}^{(2)} \qquad (i = A_1 + 1, \ldots, A - 1) \tag{27}$$

for nucleus 2. In these expressions appear the coordinates of the centres of mass of both nuclei,

$$\boldsymbol{R}_{\rm CM}^{(1)} = \frac{1}{A_1} \sum_{i=1}^{A_1} \boldsymbol{r}_i, \tag{28}$$

$$\boldsymbol{R}_{\rm CM}^{(2)} = \frac{1}{A_2} \sum_{i=A_1+1}^{A} \boldsymbol{r}_i. \tag{29}$$

Only $A_1 - 1$ coordinates $\boldsymbol{\xi}_i^{(1)}$ and $A_2 - 1$ coordinates $\boldsymbol{\xi}_i^{(2)}$ are independent. This must be taken into account in calculations of matrix elements.

The CM coordinate of both nuclei is

$$\boldsymbol{R}_{\rm CM} = \frac{1}{A}(A_1 \boldsymbol{R}_{\rm CM}^{(1)} + A_2 \boldsymbol{R}_{\rm CM}^{(2)}) = \frac{1}{A} \sum_{i=1}^{A} \boldsymbol{r}_i. \tag{30}$$

The relative coordinate between both nuclei is defined by

$$\boldsymbol{\rho} = \boldsymbol{R}_{\rm CM}^{(2)} - \boldsymbol{R}_{\rm CM}^{(1)}. \tag{31}$$

We shall see that this coordinate does only have a physical meaning when both nuclei are far apart.

Let us select two internal functions ϕ_1 and ϕ_2 describing the internal structure of clusters 1 and 2. These functions are chosen within some model and are thus known. They are approximate eigenfunctions of the internal Hamiltonians H_1 and H_2 which have the same form as (1) but with A_1 and A_2 nucleons, respectively. They are both antisymmetric and normed. Their energies are given by the variational expressions

$$E_k = \langle \phi_k | H_k | \phi_k \rangle \tag{32}$$

for $k = 1$ and 2.

The resonating-group wave function is defined as

$$\Psi = \frac{A!}{A_1! A_2!} \mathcal{A} \phi_1(\boldsymbol{\xi}_i^{(1)}) \phi_2(\boldsymbol{\xi}_j^{(2)}) g(\boldsymbol{\rho}), \tag{33}$$

where g is an unknown function of the relative coordinate. The coefficient is introduced for convenience. The assumption that nucleons with coordinates $\boldsymbol{r}_1$ to $\boldsymbol{r}_{A_1}$ belong to cluster 1 and that nucleons of coordinates $\boldsymbol{r}_{A_1+1}$ to $\boldsymbol{r}_A$ belong to cluster 2 is necessary to give a precise mathematical meaning to the notation in (33) but has no physical meaning since nucleons are indistinguishable in the isospin formalism. The difficulty with this wave function comes from the fact that the permutations P_p in the antisymmetrization projector $\mathcal{A}$ may modify the variables on which ϕ_1, ϕ_2 and g depend. Indeed, if some coordinates are permuted between clusters 1 and 2, i.e. if a nucleon of cluster 1 is exchanged with a nucleon of cluster 2, the relative coordinate $\boldsymbol{\rho}$ is transformed into a linear combination of $\boldsymbol{\rho}$ and the $\boldsymbol{\xi}_i^{(1)}$ and $\boldsymbol{\xi}_j^{(2)}$. The internal coordinates are transformed into expressions containing $\boldsymbol{\rho}$ and the internal wave functions ϕ_1 and ϕ_2 then depend on $\boldsymbol{\rho}$. Manipulating the resonating-group wave function is thus rather difficult. However, we will see in §4 that simpler calculations are also possible.

3.2 The resonating-group equation

The resonating-group method (RGM) provides a fully microscopic description of collisions. Wave function (33) is not yet adapted to a practical calculation because it does not display the good quantum numbers of the physical problem. To simplify the presentation, let us assume that the interaction between the nucleons is purely central, as in (19). Then Hamiltonian (1) commutes with $\boldsymbol{L}^2$ and $\boldsymbol{S}^2$ separately and the total orbital momentum L and the total spin S are both good quantum numbers. The total orbital-momentum operator (3) can be written as

$$\boldsymbol{L} = \boldsymbol{L}^{(1)} + \boldsymbol{L}^{(2)} + \boldsymbol{l} + \boldsymbol{L}_{\rm CM} \tag{34}$$

where $\boldsymbol{L}^{(k)}$ is the total internal orbital-momentum operator of cluster k, $\boldsymbol{l}$ is the orbital-momentum operator of the relative motion between the clusters and $\boldsymbol{L}_{\rm CM}$ is the orbital-momentum operator of the CM. If both clusters have total orbital-momentum quantum numbers $L_1 = L_2 = 0$, the total orbital momentum L of the two-cluster system is equal to the orbital momentum l of the relative motion. More general presentations can be found in [1, 2].

In this case, the RGM wave function reads

$$\Psi_{lm} = \frac{A!}{A_1!A_2!}\mathcal{A}\phi_1(\boldsymbol{\xi}_i^{(1)})\phi_2(\boldsymbol{\xi}_j^{(2)})\rho^{-1}g_l(\rho)Y_{lm}(\Omega) \tag{35}$$

where ρ and $\Omega = (\theta, \varphi)$ are the spherical coordinates of $\boldsymbol{\rho}$. It depends on an unknown radial wave function g_l for the relative motion. The antisymmetric internal wave functions ϕ_1 and ϕ_2 are normalized to unity and defined in the harmonic-oscillator shell model. For simplicity, we assume that they have a common oscillator parameter b. The variational principle is applied to Hamiltonian (1) using trial wave function (35). The unknown relative function g_l is obtained from the stationary equation

$$\langle \delta\Psi_{lm}|H - E_T|\Psi_{lm}\rangle = 0 \tag{36}$$

where the integration involves all internal coordinates and $\boldsymbol{\rho}$. The energy E_T is the total energy of the A-body system. Since ϕ_1 and ϕ_2 are fixed, the variation only affects

g_l. For an arbitrary variation δg_l, (36) becomes with (8) and (9) equivalent to

$$\langle \phi_1 \phi_2 Y_{lm} | H - E_T | \Psi_{lm} \rangle = 0 \tag{37}$$

where the integration now runs over all internal coordinates. For the study of collisions, it is more convenient to introduce the relative energy

$$E = E_T - E_1 - E_2 \tag{38}$$

where the sum $E_1 + E_2$ of the internal energies E_i of clusters $i = 1, 2$ is the *threshold energy*.

Equation (37) leads to an integro-differential equation involving local and non-local potentials [1, 2],

$$[T_l + V_D(\rho)] g_l(\rho) + \int_0^\infty \left[K_l^H(\rho, \rho') + E K_l^N(\rho, \rho') \right] g_l(\rho') d\rho' = E g_l(\rho). \tag{39}$$

In this expression, T_l is the relative kinetic energy operator

$$T_l = -\frac{\hbar^2}{2\mu} \left(\frac{d^2}{d\rho^2} - \frac{l(l+1)}{\rho^2} \right), \tag{40}$$

where $\mu = (A_1 A_2 / A) m_N$ is the reduced mass of the clusters. The local potential $V_D(\rho)$ is the *direct potential*

$$V_D(\rho) = \langle \phi_1 \phi_2 | \sum_{i=1}^{A_1} \sum_{j=A_1+1}^{A} V_{ij} | \phi_1 \phi_2 \rangle. \tag{41}$$

The non-local potentials $K_l^H(\rho, \rho')$ and $K_l^N(\rho, \rho')$ are the *Hamiltonian* and *overlap* or *norm exchange kernels*, respectively. They arise from the exchange terms of the anti-symmetrization projector, i.e. the terms that exchange nucleons between both clusters. Non-locality is thus a natural consequence of the fact that particles are indistinguishable. The complicated nonlocal potential K_l^H comprises exchange kernels for the kinetic and potential energies. The total non-local potential depends linearly on energy.

The relative wave functions g_l have no physical meaning since ρ has no physical meaning because of antisymmetrization. Functions g_l at different energies are not orthogonal.

The total wave function (35) is particularly well adapted to the treatment of scattering states. Notice however that solutions of equation (39) may also exist for bound states. The relative energy E is then negative. These bound states display a cluster structure that may not be easily described by the shell model.

3.3 Forbidden states

The notion of forbidden state can be understood with a simple atomic example. Consider an electron impinging on a helium atom. Both $1s$ orbitals are occupied in the helium ground state. If we also put the third electron in the lowest $1s$ orbital, the three-electron wave function vanishes identically. The $1s$ orbital is *forbidden* to the incoming electron. Electron scattering wave functions are orthogonal to the $1s$ orbital.

The same notion appears in nuclear physics when the nucleus is described within the shell model. Consider a neutron impinging on an α particle. In the shell-model ground state of ^{4}He, the four nucleons occupy the lowest $0s$ orbital. If the incoming neutron occupies this same orbital, the five-nucleon wave function vanishes identically. The $0s$ orbital is forbidden to the incoming nucleon.

These examples are rather obvious but it should be noticed that forbidden states occur in an approximate description of the atom or nucleus, i.e. the independent-particle model. Also within a given approximation, the notion of forbidden state can be extended to collisions between two nuclei. Let us assume that the internal wave functions ϕ_1 and ϕ_2 of two clusters are defined in the harmonic-oscillator shell model, as in the example (5) and (6). We also assume that the two clusters have the same oscillator parameter b. Forbidden states with relative wave functions g_{FS} exist and are defined by

$$\mathcal{A}\phi_1(\boldsymbol{\xi}_i^{(1)})\phi_2(\boldsymbol{\xi}_j^{(2)})\rho^{-1}g_l^{FS}(\rho)Y_{lm}(\Omega) = 0. \tag{42}$$

For these relative wave functions g_l^{FS}, the RGM wave function vanishes identically. Comparing (35) and (42), one sees that relative wave functions g_l are not defined uniquely. They may be modified by adding arbitrary amounts of forbidden states without affecting the antisymmetric RGM wave function Ψ_{lm}.

Property (42) is not satisfied for A_1, $A_2 > 1$ if the oscillator parameters of the clusters differ or if the shell-model states are not of the harmonic-oscillator type. One could thus think that the notion of forbidden state lacks generality. However, as mentioned above, these states have a physical importance (see §4.6), for reasons that are not yet fully understood. Forbidden states play an important role not only in the RGM but also in the construction of nucleon-nucleus and nucleus-nucleus potentials (§5.3). The realization of the importance of this notion has allowed to improve the description of various reactions and decay processes.

Comparing expressions (37) and (42), one observes that forbidden states are trivial solutions of (39) at all energies. By applying the same reasoning to the coefficient of E_T in (37), one obtains that the forbidden states verify the equation

$$\int_0^\infty K_l^N(\rho,\rho')g_l^{FS}(\rho')d\rho' = g_l^{FS}(\rho), \tag{43}$$

i.e. they are eigenfunctions of the norm exchange potentials with eigenvalue 1.

3.4 Resolution of the resonating-group equation

The solution g_l of the RGM equation (39) at a given energy is not unique if a forbidden state exists in the lth partial wave. The resolution of the RGM equation is thus not so easy because of the occurrence of the forbidden states. Recently however, a simple and accurate technique based on the R-matrix method has been established [7], where the problem raised by the forbidden states can be solved by eliminating poles of the R matrix. The only difference with the standard calculable R matrix occurs in the calculation of the matrix elements of the Hamiltonian and overlap. This calculation remains nevertheless rather simple with the technique of Ref. [7]. In order to use the R-matrix method, one needs to know the asymptotic behaviour of the solutions.

At large distances, Hamiltonian (1) can be written as

$$H \underset{\rho\to\infty}{\longrightarrow} H_1 + H_2 + T_{\boldsymbol{\rho}} + V_C(\rho), \tag{44}$$

where $T_{\boldsymbol{\rho}}$ is the relative kinetic-energy operator and V_C is the Coulomb potential between two charges Z_1e and Z_2e at distance ρ. This terms results from the asymptotic form of the Coulomb part of the direct potential. The direct-potential component corresponding to the nuclear interaction and all exchange kernels (including those resulting from the Coulomb interaction) have a short range and are thus negligible. They vanish when the overlap between the clusters tends to zero. At large distances, the effects of antisymmetrization between the clusters thus become negligible in the RGM wave function and $\mathcal{A}$ can be replaced by

$$\mathcal{A} \to \frac{A_1!A_2!}{A!}\mathcal{A}_1\mathcal{A}_2, \tag{45}$$

where $\mathcal{A}_1$ and $\mathcal{A}_2$ are partial antisymmetrization projectors. The wave function (35) tends to

$$\Psi_{lm} \underset{\rho\to\infty}{\longrightarrow} \phi_1\phi_2\rho^{-1}g_l(\rho)Y_{lm}(\Omega), \tag{46}$$

since $\mathcal{A}_1\phi_1 = \phi_1$ and $\mathcal{A}_2\phi_2 = \phi_2$. For large ρ values, the radial wave function g_l is a linear combination of the Coulomb wave functions F_l and G_l.

The main problem of the RGM is however not to solve (39). The main difficulty of the RGM comes from the calculation of the overlap and Hamiltonian kernels which is very complicated and not systematic. The reason is that the relative coordinate ρ and the cluster internal coordinates in (35) are modified in different ways by the different terms of operator $\mathcal{A}$. This method requires heavy analytical calculations [1, 2]. This problem is simplified by using the generator coordinate method, described in the next section.

3.5 Example: α + n elastic scattering

Before concluding this section, let us consider the example of the α + n scattering. The α internal function ϕ_1 is given by (16) with internal energy E_α. The neutron internal function ϕ_2 is just its spin-isospin state $|m_s n\rangle$ and its internal energy is zero. This system possesses one forbidden state in the s wave as expected from the discussion at the beginning of section 3.3. Its radial wave function is

$$g_0^{FS}(\rho) = (\mu'/b^2)^{3/4}\rho e^{-\mu'\rho^2/2b^2} \tag{47}$$

where $\mu' = 4/5$. This can be proved with the not so simple expression of the norm exchange kernel

$$K_l^N(\rho,\rho') = 4\pi\rho\rho'(-1)^l\left(\frac{4}{5}\right)^3\left(\frac{4}{3\pi b^2}\right)^{3/2}\exp\left[-\frac{34}{75b^2}(\rho^2+\rho'^2)\right] i_l\left(\frac{32\rho\rho'}{75b^2}\right). \tag{48}$$

In this expression, $i_l(x) = \sqrt{\pi/2x}I_{l+1/2}(x)$ where $I_{l+1/2}(x)$ is a modified spherical Bessel function of the first kind. For $l = 0$, one has $i_0(x) = \sinh x/x$. A simpler proof is given in §4.2.

With the technique of [7], α + n phase shifts can be obtained in perfect agreement with those presented in §4.5.

4 The generator-coordinate method

4.1 The generator-coordinate representation of RGM wave functions

The generator coordinate method (GCM) has provided a significant simplification of the RGM by allowing systematic calculations. The treatment of antisymmetrization can be performed by using standard techniques based on Slater determinants in a non-orthogonal basis [8]. It is only valid within the harmonic-oscillator basis. We shall also assume that the harmonic-oscillator parameters are identical.

This method is based on a link between the RGM wave function (33) and an integral transformation of a Slater determinant. Let us consider two normed Slater determinants Φ_1 and Φ_2, involving A_1 and A_2 nucleons respectively, defined in the harmonic-oscillator model and centred at two different points $\boldsymbol{R}_1$ and $\boldsymbol{R}_2$. If one antisymmetrizes their product, one obtains another Slater determinant defined in the *two-centre harmonic-oscillator shell model*,

$$\Phi = \frac{A!}{A_1!A_2!}\mathcal{A}\Phi_1(\boldsymbol{R}_1)\Phi_2(\boldsymbol{R}_2). \tag{49}$$

Although Φ_1 and Φ_2 are normed, Φ is not normed. This determinant does not vanish as long as $\boldsymbol{R}_1 \neq \boldsymbol{R}_2$. Now let us use the Bethe and Rose theorem [3] to factorize Φ_1 and Φ_2 as

$$\Phi_k(\boldsymbol{R}_k) = \varphi^{(k)}_{\rm CM}(\boldsymbol{R}^{(k)}_{\rm CM} - \boldsymbol{R}_k)\phi_k(\boldsymbol{\xi}^{(k)}_i) \tag{50}$$

for $k = 1$, 2. The internal wave functions ϕ_k are thus identical to those appearing in the RGM wave function. The CM functions are given from (15) as

$$\varphi^{(k)}_{\rm CM}(\boldsymbol{R}^{(k)}_{\rm CM} - \boldsymbol{R}_k) = (A_k/\pi b^2)^{3/4} e^{-A_k(\boldsymbol{R}^{(k)}_{\rm CM} - \boldsymbol{R}_k)^2/2b^2}. \tag{51}$$

One can write using (30) and (31),

$$A_1(\boldsymbol{R}^{(1)}_{\rm CM} - \boldsymbol{R}_1)^2 + A_2(\boldsymbol{R}^{(2)}_{\rm CM} - \boldsymbol{R}_2)^2 = AR^2_{\rm CM} + \mu'(\boldsymbol{\rho} - \boldsymbol{R})^2, \tag{52}$$

where $\mu' = A_1A_2/A$ is the reduced mass in units of the nucleon mass, if one chooses

$$\boldsymbol{R}_1 = -\frac{A_2}{A}\,\boldsymbol{R} \qquad \boldsymbol{R}_2 = \frac{A_1}{A}\,\boldsymbol{R}. \tag{53}$$

Hence, since the oscillator parameters are equal, one has

$$\varphi^{(1)}_{\rm CM}(\boldsymbol{R}^{(1)}_{\rm CM} - \boldsymbol{R}_1)\varphi^{(2)}_{\rm CM}(\boldsymbol{R}^{(2)}_{\rm CM} - \boldsymbol{R}_2) = \varphi_{\rm CM}(\boldsymbol{R}_{\rm CM})\Gamma(\boldsymbol{\rho} - \boldsymbol{R}). \tag{54}$$

where $\varphi_{\rm CM}$ is again given by the $0s$ oscillator ground-state wave function (15) and is independent of the generator coordinate, and

$$\Gamma(\boldsymbol{\rho} - \boldsymbol{R}) = (\mu'/\pi b^2)^{3/4} e^{-\mu'(\boldsymbol{\rho} - \boldsymbol{R})^2/2b^2}. \tag{55}$$

Finally, as the antisymmetrization projector commutes with the CM coordinate, (49) can be written as

$$\Phi(\boldsymbol{R}) = \frac{A!}{A_1!A_2!}\varphi_{\rm CM}\mathcal{A}\phi_1(\boldsymbol{\xi}_i^{(1)})\phi_2(\boldsymbol{\xi}_j^{(2)})\Gamma(\boldsymbol{\rho}-\boldsymbol{R}). \tag{56}$$

This expression has the same structure as the RGM wave function. Both expressions can be related by [9]

$$\varphi_{\rm CM}\Psi = \int d\boldsymbol{R} f(\boldsymbol{R})\Phi(\boldsymbol{R}). \tag{57}$$

i.e., except for a simple CM factor, the RGM wave function is obtained by an integral transform of a Slater determinant. The vector $\boldsymbol{R}$ is the *generator coordinate* and f is the *generating function*. The relative wave function is given by

$$g(\boldsymbol{\rho}) = \int d\boldsymbol{R} f(\boldsymbol{R})\Gamma(\boldsymbol{\rho}-\boldsymbol{R}). \tag{58}$$

The determination of g can be replaced by the determination of f.

The GCM is based on the link (57) between RGM wave functions and Slater determinants. Matrix elements between Slater determinants are relatively easy to obtain [8]. The calculation is based on properties (8) and (9) of the antisymmetrization projector and on properties of determinants. From now on, let us assume that the overlap and Hamiltonian matrix elements

$$N(\boldsymbol{R},\boldsymbol{R}') = \langle\Phi(\boldsymbol{R})|\Phi(\boldsymbol{R}')\rangle \tag{59}$$

and

$$H(\boldsymbol{R},\boldsymbol{R}') = \langle\Phi(\boldsymbol{R})|H|\Phi(\boldsymbol{R}')\rangle \tag{60}$$

are available. The relative simplicity of matrix elements (59) and (60) is at the basis of the GCM.

4.2 Angular-momentum projection

We have now to adapt these relations to a given partial wave. The Slater determinants can be projected on the orbital momentum l with

$$\Phi_{lm}(R) = \frac{1}{4\pi}\int d\Omega_R Y_{lm}(\Omega_R)\Phi(\boldsymbol{R}) \tag{61}$$

where $\Omega_R = (\theta_R, \varphi_R)$ represents the angular coordinates of the generator coordinate $\boldsymbol{R}$. The integral over Ω_R can be performed using the expansions

$$e^{zu} = \sum_{\lambda=0}^{\infty}(2\lambda+1)P_\lambda(u)i_\lambda(z) \tag{62}$$

with $-1 \le u \le 1$ and

$$P_\lambda(\hat{\boldsymbol{r}}\cdot\hat{\boldsymbol{r}}') = \frac{4\pi}{2\lambda+1}\sum_{\mu=-\lambda}^{\lambda} Y^*_{\lambda\mu}(\Omega_r)Y_{\lambda\mu}(\Omega_{r'}). \tag{63}$$

Introducing (56) into (61), one obtains with (62) and (63)

$$\Phi_{lm}(R) = \frac{A!}{A_1!A_2!}\varphi_{\rm CM}\mathcal{A}\phi_1(\boldsymbol{\xi}_i^{(1)})\phi_2(\boldsymbol{\xi}_j^{(2)})\Gamma_l(\rho,R)Y_{lm}(\Omega) \tag{64}$$

where appears the projected Gaussian function

$$\Gamma_l(\rho,R) = \left(\frac{\mu'}{\pi b^2}\right)^{3/4}\exp\left(-\frac{\mu'(\rho^2+R^2)}{2b^2}\right) i_l\left(\frac{\mu'\rho R}{b^2}\right). \tag{65}$$

Since the Slater determinant (49) with centres (53) vanishes for $R=0$, one obtains that $\Gamma_0(\rho,0)$ is a forbidden state. Hence, (47) is a forbidden state for any cluster system.

Matrix elements between projected Slater determinants are given by

$$N_l(R,R') = \langle\Phi_{lm}(R)|\Phi_{lm}(R')\rangle \tag{66}$$

and

$$H_l(R,R') = \langle\Phi_{lm}(R)|H|\Phi_{lm}(R')\rangle. \tag{67}$$

These expressions are obtained from $N(\boldsymbol{R},\boldsymbol{R}')$ and $H(\boldsymbol{R},\boldsymbol{R}')$ with the expansions

$$N(\boldsymbol{R},\boldsymbol{R}') = 4\pi\sum_{l=0}^{\infty}(2l+1)P_l(u)N_l(R,R') \tag{68}$$

and

$$H(\boldsymbol{R},\boldsymbol{R}') = 4\pi\sum_{l=0}^{\infty}(2l+1)P_l(u)H_l(R,R') \tag{69}$$

where $u = \hat{\boldsymbol{R}}\cdot\hat{\boldsymbol{R}}'$ is the cosine of the angle between $\boldsymbol{R}$ and $\boldsymbol{R}'$. Analytically, expansions (68) and (69) are easily obtained with formula (62). Numerically, (66) can be obtained from the inverse of (68),

$$N_l(R,R') = \frac{1}{8\pi}\int_{-1}^{+1}P_l(u)N(\boldsymbol{R},\boldsymbol{R}')du, \tag{70}$$

and $H_l(R,R')$ from a similar expression.

Finally, let us note that these matrix elements are related to the RGM exchange kernels by

$$N_l(R,R') = \int_0^\infty \rho d\rho\int_0^\infty \rho' d\rho'\,\Gamma_l(\rho,R)\left[\delta(\rho-\rho') - K_l^N(\rho,\rho')\right]\Gamma_l(\rho',R') \tag{71}$$

and a similar relation for $H_l(R,R')$. However, relation (71) has little practical importance because K_l^N is much more complicated to derive than N_l. The inversion of (71) has been used to derive explicit kernels for the RGM equation but it is only feasible analytically [9, 2]. The kernels N_l and H_l can be derived either analytically or numerically.

4.3 The Griffin-Hill-Wheeler equations

In the GCM, the relative wave function $g_l(\rho)$ can thus be expanded over projected Gaussian functions as

$$g_l(\rho) = \int_0^\infty f_l(R)\Gamma_l(\rho, R)dR, \tag{72}$$

where R is the generator coordinate. The calculation of $g_l(\rho)$ can therefore be replaced by the calculation of the generating function $f_l(R)$.

Inserting (72) in the RGM definition (35) provides

$$\varphi_{\rm CM}\Psi_{lm} = \int_0^\infty f_l(R)\Phi_{lm}(R)dR, \tag{73}$$

After multiplication by an appropriate factor depending on the CM coordinate of the A nucleons, the RGM wave function $\Psi_{lm}(R)$ can be expressed as a function of projected Slater determinants provided that the oscillator parameters of the clusters are identical. This property is well adapted to systematic numerical calculations since the calculation of matrix elements (59) and (60) involves single-particle orbitals only. The projection (70) on the angular momentum l can be performed numerically. The presence of the CM factor does not affect the matrix elements.

The generating function f_l is solution of the Griffin-Hill-Wheeler equation [10]

$$\int_0^\infty [H_l(R, R') - EN_l(R, R')]f_l(R')dR' = 0. \tag{74}$$

However this equation is not easy to solve for a scattering problem and f_l is not a well-behaved function (in fact, it is not a function but rather a distribution).

In practice, the integral in (72) is replaced by a finite sum over a set of values R_n of the generator coordinate. This means that, at large distances ρ, the radial wave function g_l presents a Gaussian behaviour, not consistent with the physical asymptotic behaviour of a scattering wave function. This problem can be addressed by using the microscopic R-matrix method which adapts the R-matrix formalism to antisymmetrized wave functions.

4.4 The microscopic R-matrix method

In the microscopic R-matrix method [11], the wave function is approximated in the internal region by a discretized version of (73) as

$$\varphi_{\rm CM}\Psi^{\rm int}_{lm} = \sum_{n=1}^{N} f_l(R_n)\Phi_{lm}(R_n). \tag{75}$$

In the external region, it is approximated by the asymptotic expression (46) as

$$\Psi^{\rm ext}_{lm} \;=\; \phi_1\phi_2\rho^{-1}g^{\rm ext}_l(\rho)Y_{lm}(\Omega) \tag{76}$$

where the external radial function $g^{\rm ext}_l$ is a linear combination of Coulomb functions.

The application of the R-matrix method to the GCM is straightforward. The calculation involves matrix elements of the Hamiltonian evaluated over the internal

region only. This is achieved by subtracting the external contributions. By definition of the channel radius a, antisymmetrization effects and the nuclear interaction are negligible in the external region. The relevant matrix elements are therefore given by

$$\langle \Phi_{lm}(R_n)|\Phi_{lm}(R_{n'})\rangle_{\rm int} = N_l(R_n,R_{n'}) - \int_a^\infty \Gamma_l(\rho,R_n)\Gamma_l(\rho,R_{n'})\rho^2 d\rho, \qquad (77)$$

$$\langle \Phi_{lm}(R_n)|H|\Phi_{lm}(R_{n'})\rangle_{\rm int} = H_l(R_n,R_{n'}) - \int_a^\infty \rho\Gamma_l(\rho,R_n)(T_l + V_C(\rho) + E_1 + E_2)\rho\Gamma_l(\rho,R_{n'})d\rho, \qquad (78)$$

where the first terms in the r.h.s. are matrix elements (66) and (67) calculated over the whole space. The second terms represent the external contributions of the basis functions (64). They can easily be computed numerically. Then the R-matrix and the associated collision matrix are obtained as in the standard calculable R matrix [11, 12]. The collision matrix should not depend on the choice of the channel radius a, provided it is large enough to make not only the nuclear interaction but also the antisymmetrization effects negligible in the external region.

Another interesting aspect of the GCM is that, contrary to the RGM, forbidden states do not cause any problem.

4.5 Examples: α + n and $\alpha + \alpha$ elastic scatterings

The first example concerns the relatively simple α + n scattering. The GCM basis functions (49) read

$$\Phi = 5\mathcal{A}\Phi_\alpha(-\frac{1}{5}\boldsymbol{R})\Phi_n(+\frac{4}{5}\boldsymbol{R}), \qquad (79)$$

where Φ_α is given by (5) with its location shifted and Φ_n is the product of a shifted (6) by $|m_s n\rangle$. The overlap matrix element is given by

$$N(\boldsymbol{R},\boldsymbol{R}') = \exp\left(-\frac{1}{5b^2}(\boldsymbol{R}-\boldsymbol{R}')^2\right)\left[1-\exp\left(-\frac{1}{2b^2}\boldsymbol{R}\cdot\boldsymbol{R}'\right)\right]. \qquad (80)$$

The α + n scattering is described with an α-cluster internal wave function ϕ_α defined with an oscillator parameter $b = 1.36$ fm. The microscopic R-matrix method is employed for the numerical calculations with the Minnesota effective interaction (19) as central nucleon-nucleon force and a zero-range spin-orbit force (22). With the Minnesota force, the binding energy of the α particle is 24.28 MeV, which is smaller than the experimental value 28.30 MeV. The admixture parameter u is taken as $u = 0.96$. The spin-orbit parameter $S_0 = 35.6$ MeV fm^5 is used for the p waves. The calculation is performed with $N = 10$ basis functions in (75) with R_n values ranging from 0.4 fm to 8.5 fm by steps of 0.9 fm and $a = 7.6$ fm [13].

The $l = 0$ ($J^\pi = 1/2^+$) and $l = 1$ ($J^\pi = 1/2^-$ and $3/2^-$) phase shifts are displayed in Fig. 1. The $p3/2$ phase shift presents a broad resonance, the $3/2^-$ ground state of ^{5}He. An even broader $p1/2$ resonance corresponds to the $1/2^-$ first excited state. The $s1/2$ phase shift is non resonant. A comparison showing the excellent agreement between the RGM and GCM can be found for the α + n scattering in [7].

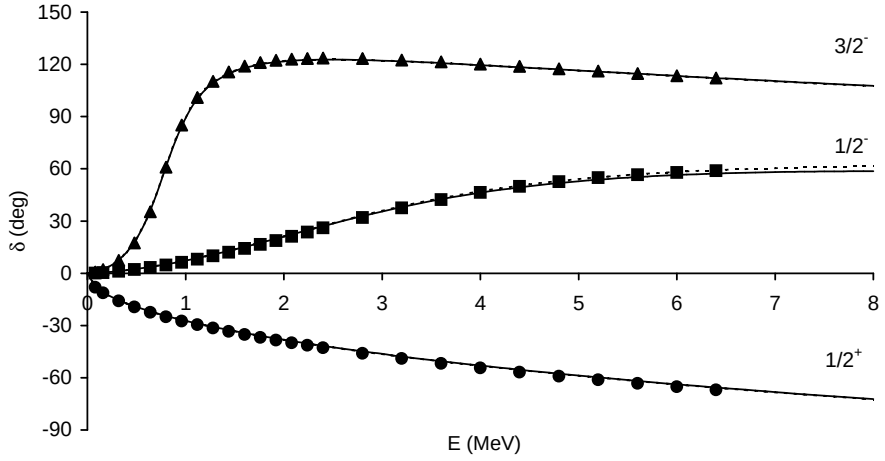

Figure 1: α + n GCM phase shifts calculated with the Minnesota interaction (full lines) compared with phase shifts extracted from experiment (see [13] for details).

The second example deals with the $\alpha + \alpha$ system. The GCM basis functions read

$$\Phi = \frac{8!}{4!^2}\mathcal{A}\Phi_\alpha(-\frac{1}{2}\boldsymbol{R})\Phi_\alpha(+\frac{1}{2}\boldsymbol{R}). \tag{81}$$

The overlap matrix element is given by

$$N(\boldsymbol{R},\boldsymbol{R}') = \left[\exp\left(-\frac{1}{2b^2}(\boldsymbol{R}-\boldsymbol{R}')^2\right) - \exp\left(-\frac{1}{2b^2}(\boldsymbol{R}+\boldsymbol{R}')^2\right)\right]^4. \tag{82}$$

Since it is a system of two identical bosons, the RGM wave function must be symmetric with respect to their exchange, i.e. for $\boldsymbol{\rho} \to -\boldsymbol{\rho}$. Since the spherical harmonics in (35) have a parity $(-1)^l$, all odd-l waves are forbidden. This property can be checked by observing with (82) and (62) that $N_l(R,R')$ and also $H_l(R,R')$ vanish identically for l odd because of the symmetry for $\boldsymbol{R}' \to -\boldsymbol{R}'$.

This system possesses three forbidden states: two in the s wave and one in the d wave. Both α clusters are described by internal wave functions ϕ_α defined in (16) with an oscillator parameter $b = 1.36$ fm. The Minnesota interaction is used with an admixture parameter $u = 0.94687$. This value provides an excellent description of the $\alpha+\alpha$ phase shifts over a broad energy range [14]. The microscopic R-matrix calculation is performed with $N = 10$ basis functions with R_n values ranging from 0.8 fm to 8 fm by steps of 0.8 fm. In Table 2 are given the $l = 0$ phase shifts at typical energies for various conditions of calculation [12]. The channel radius a is taken as $a = 6.4$ fm or $a = 7.2$ fm and $N = 9$ is also considered. In all cases, the phase shifts are very stable when the conditions are changed. They are obtained with an accuracy better than 0.1°.

Fig. 2 shows the phase shifts as a function of energy [12]. The cluster model is well adapted to the $\alpha+\alpha$ system since the first reaction threshold (^{7}Li+p) is near 17 MeV.

The GCM phase shifts are therefore in very good agreement with experiment. The narrow ground-state resonance located at 92 keV is not observable at the scale of the figure. Broad resonances appear in the d wave near 3 MeV and in the g wave near 13 MeV.

Table 2: Microscopic $\alpha + \alpha$ phase shifts (in degrees) for different conditions of calculation [12].

E (MeV)	$N = 9$		$N = 10$	
	$a = 6.4$ fm	$a = 7.2$ fm	$a = 6.4$ fm	$a = 7.2$ fm
1	146.00	145.93	146.00	146.00
5	47.48	47.42	47.49	47.48
10	−5.67	−5.79	−5.67	−5.67
15	−38.47	−38.52	−38.46	−38.46

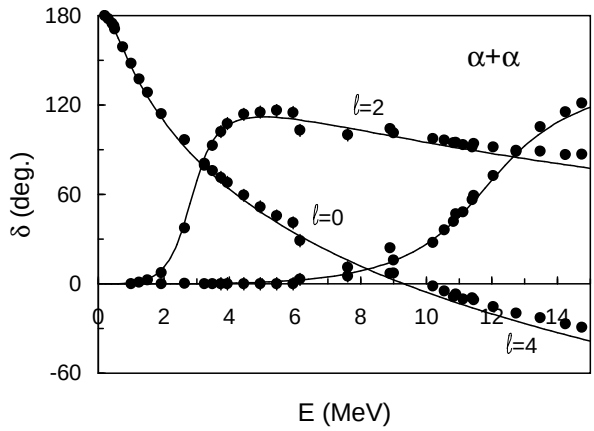

Figure 2: $\alpha+\alpha$ GCM phase shifts calculated with the Minnesota interaction (full lines) compared with a phase shift analysis (see [12] for details).

4.6 The Levinson theorem

The Levinson theorem gives the variation of the phase shift when the energy varies from zero to infinity. In local-potential scattering, it reads

$$\delta_l(0) - \delta_l(\infty) = n_l \pi, \tag{83}$$

where n_l is the number of bound states in partial wave l. For non-local potentials, this theorem must be modified into [15]

$$\delta_l(0) - \delta_l(\infty) = (n_l + m_l)\pi, \tag{84}$$

where m_l is the number of forbidden states in partial wave l.

The α + n system does not have any bound state: ^{5}He is particle unstable. Only one forbidden state (47) exists in the s wave ($m_0 = 1$). For the $l \neq 0$ partial waves, expression (83) remains thus valid. For the s wave, $\delta_0(0)$ and $\delta_0(\infty)$ differ by π. For $\delta_0(0) = 0$, the phase shift must tend to $-\pi$, in agreement with its behaviour in Fig. 1.

The α + α system has also no bound state since ^{8}Be is particle unstable. Two forbidden states exist in the s wave ($m_0 = 2$) and one forbidden state exists in the d wave ($m_2 = 1$). The phase shift δ_0 jumps from 0 to π at the narrow ^{8}Be ground-state resonance, then decreases and becomes negative. It must tend towards -2π. The phase shift δ_2 displays a broad resonance and must tend towards $-\pi$.

Since forbidden states only exist under the restricted condition of the harmonic-oscillator model with equal size parameters, one might think that form (83) of the Levinson theorem is more realistic than form (84). The contrary has been shown in a model with spherical non-Gaussian α clusters [16].

5 Variants and approximations

5.1 RGM potential

The RGM equation (39) can be written more formally in operator notation as

$$(T_l + V_D + \mathcal{K}_l^H + E\mathcal{K}_l^N)g_l = Eg_l \tag{85}$$

where T_l is given by (40), V_D is the direct potential (41) and $\mathcal{K}_l^H$ and $\mathcal{K}_l^N$ are the norm and overlap integral operators. Let us introduce the norm kernel operator

$$\mathcal{N}_l = 1 - \mathcal{K}_l^N. \tag{86}$$

Equation (85) becomes

$$\mathcal{H}_l g_l = E\mathcal{N}_l g_l \tag{87}$$

with

$$\mathcal{H}_l = T_l + V_D + \mathcal{K}_l^H. \tag{88}$$

The Pauli forbidden states satisfy equation (43),

$$\mathcal{K}_l^N g_l^{FS} = g_l^{FS} \tag{89}$$

or, equivalently,

$$\mathcal{N}_l g_l^{FS} = 0. \tag{90}$$

With (87), one verifies that

$$\mathcal{H}_l g_l^{FS} = 0 \tag{91}$$

is also true.

The eigenvalue problem

$$\mathcal{K}_l^N \varphi_{nl} = \mu_{nl} \varphi_{nl} \tag{92}$$

can sometimes be solved analytically [9]. For the α + n system described in §4.5, the eigenvalues are

$$\mu_{nl} = \left(-\frac{1}{4}\right)^{2n+l}. \tag{93}$$

For the α + α system described in §4.5, they are

$$\mu_{nl} = 4\left(\frac{1}{2}\right)^{2n+l} - 3\delta_{n0}\delta_{l0} \tag{94}$$

with l even. The eigenfunctions φ_{nl} are harmonic-oscillator radial functions [9]. The Pauli forbidden states g_l^{FS} are nothing but eigenstates φ_{nl} of the norm exchange kernel $\mathcal{K}_l^N$ with eigenvalues $\mu_{nl} = 1$.

Let us introduce renormalized relative functions

$$\hat{g}_l = \mathcal{N}_l^{1/2} g_l. \tag{95}$$

This function is orthogonal to the forbidden states. Equation (87) can be converted into an equation involving an energy-independent potential,

$$(T_l + V_l^{RGM})\hat{g}_l = E\hat{g}_l. \tag{96}$$

The nonlocal potential reads

$$V_l^{RGM} = \mathcal{N}_l^{-1/2}\mathcal{H}_l\mathcal{N}_l^{-1/2} - T_l = \mathcal{N}_l^{-1/2}(T_l + V_D + \mathcal{K}_l^H)\mathcal{N}_l^{-1/2} - T_l, \tag{97}$$

where operator $\mathcal{N}_l^{-1/2}$ is defined over the Pauli allowed space, i.e. it does not involve forbidden states, otherwise the inverse would not exist. Operator $\mathcal{N}_l^{-1/2}$ is given by

$$\mathcal{N}_l^{-1/2} = \sum_{n>m_l} (1-\mu_{nl})^{-1/2} |\varphi_{nl}\rangle\langle\varphi_{nl}| \tag{98}$$

where $|\varphi_{nl}\rangle\langle\varphi_{nl}|$ is the projector on the subspace corresponding to n and l. The m_l forbidden states are excluded from the sum.

The RGM potential is a complicated non-local operator which contains effects from the kinetic and potential energies. Equation (96) leads to exactly the same bound-state energies and phase shifts as (85). It presents the advantage that functions $\hat{g}_l$ are defined uniquely and that functions corresponding to different energies are orthogonal. The functions $\hat{g}_l$ resemble much more physical radial functions than the RGM relative functions g_l. The RGM potentials V_l^{RGM} can be interpreted as effective cluster-cluster interactions. They have been used in three-body calculations [14].

5.2 Orthogonality-condition model

Equation (96) is not more practical to use than the RGM equation and even more difficult to establish. However, it leads to various interesting approximations. The basic idea is to replace the complicated non-local potential (97) by a local approximation while keeping the influence of the forbidden states. The orthogonality-condition model (OCM) is based on this idea [17].

In the OCM, (96) is replaced by

$$(T_l + V_l^{\mathrm{OCM}})\tilde{g}_l = E\tilde{g}_l \tag{99}$$

with the condition

$$\langle g_l^{FS}|\tilde{g}_l\rangle = 0 \tag{100}$$

for all forbidden states. The potential is in general adjusted to some physical properties of the system. In some cases, its dependence on l is weak and can be suppressed.

A variant of (99) and (100) reads

$$\Lambda_l(T_l + V_l^{\mathrm{OCM}})\hat{g}_l = E\hat{g}_l \tag{101}$$

where

$$\Lambda_l = \sum_{n>m_l} |\varphi_{nl}\rangle\langle\varphi_{nl}| = 1 - \sum_{FS} |g_l^{FS}\rangle\langle g_l^{FS}| \tag{102}$$

is a projector on the allowed states.

5.3 Deep potentials

Though less involved than the RGM, the OCM is still rather complicated. A simpler model that one could name *local OCM* has most of its advantages. Equation (101) is replaced by the local equation

$$(T_l + V_l)u_l = Eu_l, \tag{103}$$

where V_l is a deep local potential which contains m_l non-physical bound states below the n_l physical bound states of the lth partial wave. The idea is that the non-physical bound states should resemble the forbidden states [18]. Because the physical bound states and the scattering states are automatically orthogonal to the deep bound states, they will resemble states orthogonal to forbidden states. Because of the m_l unphysical bound states, the Levinson theorem (84) is simulated by expression (83). For each partial wave, the potential is adjusted to important physical data with the constraint to be deep enough to have m_l additional bound states. This simple model has proved remarkably successful and efficient. In some cases, the dependence on the relative orbital momentum l can even be neglected.

This model is very successful for the $\alpha + \alpha$ scattering where a simple Gaussian potential, independent of l, with only two parameters is able with a Coulomb term to reproduce the $\alpha + \alpha$ phase shifts up to 20 MeV for the $l = 0$ to 6 partial waves

[18]. This potential has two "forbidden" deep bound states in the s wave and nicely reproduces the physical ground-state resonance and its width. The ground-state wave function u_0 possesses two nodes at small distances due to the orthogonality to the non-physical bound states. Thanks to these nodes, it resembles qualitatively the RGM function $\hat{g}_0$. One "forbidden" deep bound state is present in the d wave. This deep potential gives as good a fit as an l-dependent shallow potential, without any bound states, where nine parameters are needed [19]. The relation between these two types of potential can be described mathematically [20].

Deep potentials provide successful approximations in applications where the node structure of the wave functions plays an important physical role.

5.4 Determination of the number of forbidden states

The number of forbidden states is a useful information, for example to derive deep potentials. It can be obtained with relatively simple calculations avoiding the resolution of (43) or (92).

The GCM basis functions (49) vanish when the generator coordinate R is equal to zero since one or several orbitals are occupied twice. Hence, the GCM norm kernel also vanishes when $R \to 0$ according to

$$N(\boldsymbol{R}, \boldsymbol{R}) \underset{R\to 0}{\sim} R^{2\nu} \tag{104}$$

where ν is an integer. Similarly, the projected norm kernels behave for $R \to 0$ as

$$N_l(R, R) \underset{R\to 0}{\sim} R^{2\nu_l}. \tag{105}$$

where the integers ν_l can be obtained from analytical expressions or from numerical values. One can show that the number m_l of forbidden states is given by [21]

$$m_l = \tfrac{1}{2}(\nu_l - l). \tag{106}$$

This property can be verified with (80) and (82).

References

[1] K. Wildermuth and Y. C. Tang, A Unified Theory of the Nucleus (Vieweg, Braunschweig, 1977)

[2] Y. C. Tang, in Topics in Nuclear Physics II, Lecture Notes in Physics 145 (Springer, Berlin, 1981) p.572

[3] H.A. Bethe and M.E. Rose, Phys. Rev. 51 (1937) 283

[4] A. B. Volkov, Nucl. Phys. 74 (1965) 33

[5] D. R. Thompson, M. LeMere and Y.C. Tang, Nucl. Phys. A286 (1977) 53

[6] J.A. Wheeler, Phys. Rev. 52 (1937) 1083, 1107

[7] M. Hesse, J. Roland and D. Baye, Nucl. Phys. A709 (2002) 184

[8] D. Brink, Proc. Int. School "Enrico Fermi" 36, Varenna 1965 (Academic Press, New-York, 1966) p.247

[9] H. Horiuchi, Prog. Theor. Phys. Suppl. 62, 90 (1977).

[10] D.L. Hill and J.A. Wheeler, Phys. Rev. 89 (1953) 1102

[11] D. Baye, P.-H. Heenen and M. Libert-Heinemann, Nucl. Phys. A291 (1977) 230

[12] P. Descouvemont and D. Baye, Rep. Prog. Phys. 73 (2010) 036301

[13] R. Kamouni and D. Baye, Nucl. Phys. A791 (2007) 68

[14] M. Theeten, H. Matsumura, M. Orabi, D. Baye, P. Descouvemont, Y. Fujiwara and Y. Suzuki, Phys. Rev. C 76 (2007) 054003

[15] P. Swan, Proc. Roy. Soc. A 228 (1955) 10

[16] M. Kruglanski and D. Baye, Nucl. Phys. A548 (1992) 39

[17] S. Saito, Prog. Theor. Phys. Suppl. 62 (1977) 11

[18] B. Buck, H. Friedrich and C. Wheatley, Nucl. Phys. A275 (1977) 246

[19] S. Ali and A.R. Bodmer, Nucl. Phys. 80 (1966) 99

[20] D. Baye, Phys. Rev. Lett. 58 (1987) 2738

[21] D. Baye and P.-H. Heenen, Nucl. Phys. A283 (1977) 176